phys. stat. sol. (b) **224**, No. 1, 307–312 (2001)

Photoelectrochemical Characterization of Nanocrystalline ZnS : Mn^{2+} Layers

J. F. SUYVER[1]), R. BAKKER, A. MEIJERINK, and J. J. KELLY

Debye Institute, Physics and Chemistry of Condensed Matter, Utrecht University, P.O. Box 80.000, NL-3508 TA Utrecht, Netherlands

(Received July 31, 2000; accepted October 2, 2000)

Subject classification: 72.40.+w; 78.55.Et; 78.55.Mb; 78.67.Bf; S8.11

Measurements of the photoelectrochemical properties of nanocrystalline ZnS electrodes doped with Mn^{2+} are presented and discussed. The observation of both anodic and cathodic photocurrent is direct evidence for the nanocrystalline nature of the system. In-situ photoluminescence measurements showed stable Mn^{2+} related photoluminescence over a large potential range. Due to the unfavourable kinetics of electron and hole transfer across the interface between the nanocrystallites and solution, it is concluded that recombination accounts for most of the charge carriers generated by illumination. Breakdown of the ZnS into elementary Zn and S^{2-} in solution was also observed at negative potential. This breakdown introduces new non-radiative decay paths and is responsible for the slow luminescence decrease as a function of operating time.

1. Introduction Research on electroluminescent devices has started to focus on nanocrystalline composite materials [1–3]. The main reasons for the increasing interest in these materials are, on the one hand, the simple fabrication of (doped) semiconductor nanocrystals [4, 5] and, on the other hand, the fact that in combination with a suitable semiconducting polymer and conducting substrate electrons and holes can be injected directly into the conduction and valence bands of the nanocrystals [2, 6]. This might allow for an electroluminescent device based on doped semiconductor nanocrystals.

In this paper the preparation of layers based on Mn^{2+} doped ZnS nanocrystals (NC) is described. Photoelectrochemical methods are used to characterize the layers. In particular photocurrent–potential and in-situ photoluminescence (PL) measurements can be used to show that the layers have properties typical of a nanoparticulate matrix. Electrochemical degradation of the nanocrystals was also measured and the mechanism is discussed.

2. Experimental The inorganic synthesis used to prepare ZnS : Mn^{2+} nanocrystals is similar to that described in the literature [7]. All steps of the synthesis were performed at room temperature and under conditions of ambient pressure and atmosphere. A capping polymer was used to prevent particle agglomeration. For this purpose, 10.2 g of $Na(PO_3)_n$ was dissolved in 80 ml of ultrapure water ($R \approx 16$ MΩ). While the solution was stirred, 10 ml of a 1 M $Zn(CH_3COO)_2 \cdot 2H_2O$ solution was added and allowed to mix, followed by 10 ml of a 0.1 M $MnCl_2 \cdot 4H_2O$ solution and, after a few minutes stirring, 10 ml of a 1 M $Na_2S \cdot 9H_2O$ solution. A white opaque solution resulted. After centrifuging and washing the particles twice with ultrapure water a ZnS : Mn^{2+} suspension in water was obtained. As a substrate, a 600 nm layer of SnO_2 : F (TFO) on glass

[1]) Corresponding author; Tel.: +31-30-253 2241; Fax: +31-30-253 2403; e-mail: j.f.suyver@phys.uu.nl

was used. The TFO had a surface resistance of 7 $\Omega/\Box$ and was transparent throughout the visible range. Glass plates of $(1\times3)\,cm^2$ were dipcoated 15 times from the $ZnS:Mn^{2+}$ suspension at a lift-rate of 0.5 mm/s while the suspension was slowly mixed. The dipcoated electrodes were given a mild temperature treatment for one hour at 200 °C to improve adhesion of the nanocrystals to the TFO layer and increase the surface uniformity.

After the electrodes were dipcoated, the remaining suspension was centrifuged and washed once with ethanol. The particles were again centrifuged and left to dry in a vacuum desiccator for at least 15 hours. This resulted in a fine powder with a white color.

To determine the particle diameter, X-ray powder diffraction spectra were measured with a Philips PW 1729 X-ray diffractometer using Cu K_α radiation at a wavelength of 1.542 Å. The X-ray diffraction (XRD) spectrum showed broad peaks at positions that are in good agreement with the zincblende modification of ZnS [8].

The (photo)electrochemical measurements were carried out in a conventional three-electrode cell using an EG&G model 366A potentiostat. The electrolyte was a 0.5 M solution of Na_2SO_3. Optical excitation of the electrodes was obtained using a 300 W Oriel Hg-Xe lamp in combination with a bandpass filter (250 to 390 nm, Schott model UG11-3). In-situ photoluminescence emission spectra were obtained using a Princeton Instruments liquid nitrogen cooled CCD camera (1024×256 pixels) in combination with an Acton Pro monochromator (150 lines/mm, blazed at 500 nm). A longpass filter (cutoff at 410 nm) was used to remove the excitation light. SEM measurements were performed using a Philips XL30 FEG electron microscope.

3. Results and Discussion Several reference measurements on the NC and the electrodes were performed. The average particle diameter was calculated from the broadening of the XRD lines [9], and found to be typically 4.6 nm. This value is well within the quantum-size regime, where the physical properties of the nanocrystal are highly size-dependent [2]. The transmission of the electrodes was high up to the onset of the ZnS absorption, which indicates high quality electrodes with few impurities. The electrodes showed no sign of degradation, as similar results were obtained with a three-week-old electrode, stored in ambient air, and a fresh electrode.

Figure 1 shows a voltammogram for a $ZnS:Mn^{2+}$ electrode measured while the potential was scanned from 0.3 V to −1.2 V and back to 0.3 V. During the potential scan the light source was turned on and off every 0.1 V in order to distinguish between the dark current, curve (a), and the photocurrent, curve (b).

The observed dark current can be explained by the reduction of water and oxygen (at negative potential) and the oxidation of SO_3^{2-} and water (at positive potential). These reactions probably occur mainly at the TFO surface because the $ZnS:Mn^{2+}$ layer is highly porous. There is evidence for the reduction of ZnS at negative potentials, as will be shown below. No oxidation of ZnS is expected, because the hole density in the ZnS nanocrystals in the dark is negligible.

As can be seen from Fig. 1, both an anodic photocurrent (PC) (22 $\mu A/cm^2$) and a cathodic PC (40 $\mu A/cm^2$) are observed. The contribution of the TFO layer to the photocurrent was found to be negligible.

Figure 2 shows the results of in-situ photoluminescence measurements. The inset is a spectrum measured at 0 V (SCE) and shows a peak at ≈600 nm which is attributed to the $^4T_1 \rightarrow {}^6A_1$ transition in the Mn^{2+} ion [11]. The much weaker band at ≈420 nm is

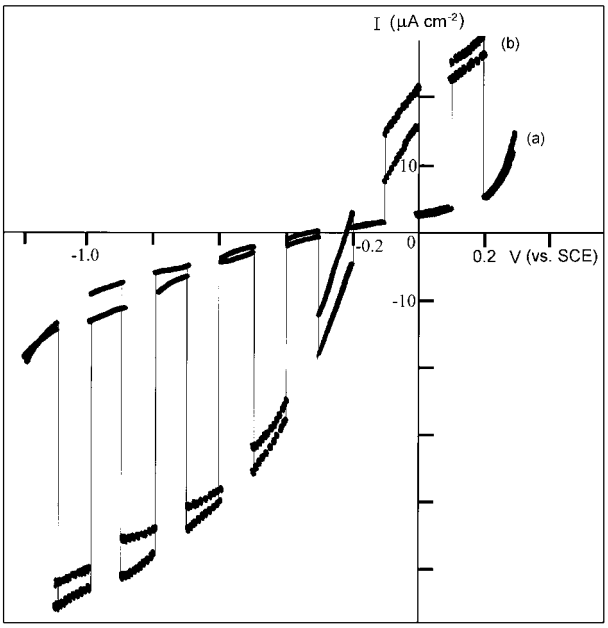

Fig. 1. Cyclic voltammogram of a 1 cm^2 $ZnS:Mn^{2+}$ electrode using a chopped light source measured (a) in the dark and (b) under illumination. A saturated calomel electrode (SCE) was used as reference

attributed to a defect-related luminescence of the ZnS host lattice [12]. The cut-off of this peak at 410 nm is due to a filter that was used during these measurements. When the potential of the electrode was scanned, this spectrum did not change in form and only the intensity varied.

The data presented in Fig. 2 show that over the whole potential range only a slight (3%) dependence of the Mn^{2+} related PL (λ = 600 nm) is observed. The decrease of the PL intensity at negative potential is almost completely restored at positive potential and only a very small permanent decrease of the PL intensity is observed. However, long-term experiments have shown that this permanent decrease continues and repeated scanning of the potential for 8 h resulted in a 50% decrease of the PL.

In a bulk n-type single crystal or polycrystalline electrode under depletion conditions photogenerated electrons and holes are separated by the electric field of the space-

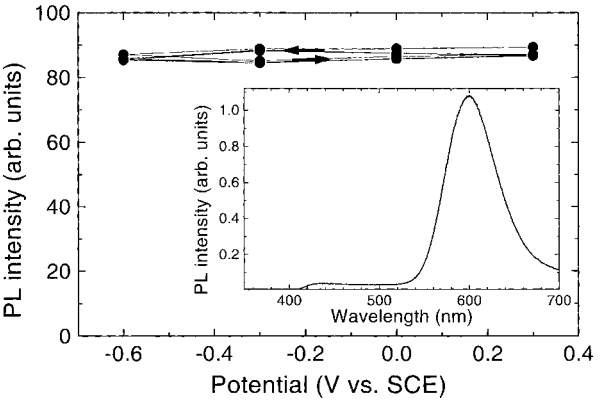

Fig. 2. In-situ photoluminescence measurement showing the dependance on applied voltage of the Mn^{2+} related photoluminescence intensity (λ = 600 nm). The lines are drawn to guide the eye. Inset: PL spectrum at 0 V (SCE). An excitation wavelength-band from 250 to 390 nm was used

charge layer. The holes migrate to the surface where they oxidize a species in solution or the semiconductor itself. The electrons are registered as an anodic PC in the external circuit. Obviously since electrons and holes are separated no PL can be observed in this case.

Close to the flat band potential the concentration of majority carriers at the surface is high and one generally observes a reduction reaction and thus a cathodic dark current due to electrons. Minority carriers generated by light recombine effectively with majority carriers. The PC becomes negligible and PL is observed in this case.

The data presented in Figs. 1 and 2 show that the results obtained with $ZnS:Mn^{2+}$ nanoparticulate layers are quite different from those described above for bulk electrodes. In a nanoparticulate electrode electrons and holes are generated within a nanocrystal. The dimensions of such crystallites are much too small to allow for the formation of a depletion layer. The electron and hole are not spatially separated and there is a high probability for recombination. If this process is radiative, then photoluminescence is observed even at positive potentials, which for a bulk electrode corresponds to (strong) depletion. The emission intensity in the case of a nanoparticulate electrode is, in contrast to a bulk electrode, essentially independent of potential in a wide range. This is clearly the case in the experiment that is shown in Fig. 2.

Because of the small dimensions of nanocrystallites, both electrons and holes in a nanoparticulate electrode can easily diffuse to the interface with the solution [1]. If there is an effective hole scavenger present in the solution and the potential applied to the electrode is such that electrons can be removed via the conducting substrate, then an anodic photocurrent is observed. This is the case in Fig. 1 at positive potential. The surface hole reaction is very likely the oxidation of SO_3^{2-}.

On the other hand, if the photogenerated electrons react at the interface with the solution and the holes are removed via the back contact then a cathodic photocurrent results. This is seen at negative potentials in Fig. 1. The reaction responsible for the cathodic photocurrent is probably reduction of oxygen present in solution.

While the anodic and cathodic photocurrent densities shown in Fig. 1 are significant, they are nevertheless small compared with what would be expected on the basis of the photon flux used. Clearly, the kinetics of electron and hole transfer across the interface between the nanocrystallites and solution are unfavourable compared to the kinetics of electron–hole recombination. Therefore, it is concluded that recombination accounts for most of the charge carriers generated by illumination.

The gradual permanent decrease in the luminescence intensity is attributed to the breakdown of the ZnS nanocrystals.

Figure 3a shows the electrode before electrochemical measurements were performed. The non-uniformity is attributed to agglomerated nanocrystals and capping polymer. The surface structure is altered significantly when the electrode potential was continuously scanned for 8 h, as can be seen from Fig. 3b. The main features remain the same as before the treatment. However, a large number of small black dots are formed on the surface. Elemental SEM analysis indicated high zinc concentrations in these dots. These results are consistent with two reactions:

$$\text{negative potential:} \quad ZnS + 2e^- \rightarrow Zn + S^{2-}\,, \tag{1}$$

$$\text{positive potential:} \quad Zn + H_2O + 2h^+ \rightarrow ZnO + 2H^+\,. \tag{2}$$

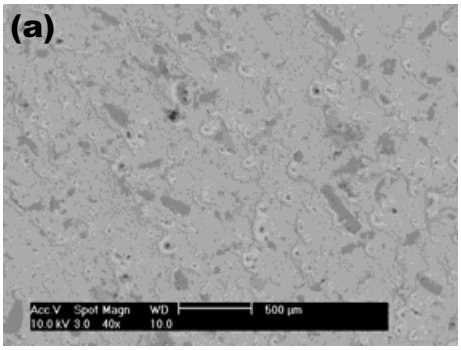

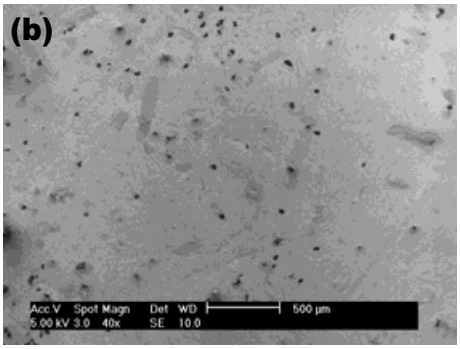

Fig. 3. SEM measurements of a $ZnS:Mn^{2+}$ electrode a) before and b) after the electrochemical treatment as discussed in the text

Reaction (1), the reduction of ZnS at negative potential, will result in the formation of elementary zinc on the surface and S^{2-} in solution. At positive potential, most of the surface-bound zinc is oxidized (reaction (2)). This process will limit the long-term stability of the electrode. This surface degradation gives rise to non-radiative (surface) recombination centres which leads to a permanent decrease of the luminescence.

4. Conclusions As far as the authors are aware, this paper presents the first potential dependent PL results on nanocrystalline $ZnS:Mn^{2+}$. Photocurrent–potential and in-situ PL measurements were used to show that the $ZnS:Mn^{2+}$ layers have properties typical of a nanoparticulate matrix. The electrodes show both anodic and cathodic photocurrent, as is expected for a nanocrystalline electrode. The small photocurrent quantum efficiency indicates that the kinetics of electron and hole transfer across the interface between the nanocrystallites and solution are unfavourable compared to the kinetics of electron–hole recombination. This is corroborated by the fact that the Mn^{2+} related luminescence is observed over a broad potential range and only small changes in the luminescence intensity are detected for each successive potential cycle. Therefore, it is concluded that electron–hole recombination accounts for most of the charge carriers generated by illumination. Potential-induced breakdown of nanocrystals is observed and explained.

Acknowledgements Dr. X. Xia is acknowledged for his help with the scanning electron microscope measurements. This work is part of the Research Program of the Priority Program for new Materials (PPM) and was made possible by financial support from the Dutch association for scientific research (NWO).

References

[1] G. Hodes, I. D. J. Howell, and L. M. Peter, J. Electrochem. Soc. **139**, 3136 (1992).
[2] N. C. Greenham, X. Peng, and A. P. Alivisatos, Phys. Rev. B **54**, 17628 (1996).
[3] J. Leeb, V. Gebhardt, G. Müller, D. Haarer, D. Su, M. Giersig, G. McMahon, and L. Spanhel, J. Phys. Chem. B **103**, 7839 (1999).
[4] K. Sooklal, B. S. Cullum, S. M. Angel, and C. J. Murphy, J. Phys. Chem. **100**, 4551 (1996).

[5] A. VAN DIJKEN, A. H. JANSSEN, M. H. P. SMITSMAN, D. VANMAEKELBERGH, and A. MEIJERINK, Chem. Mater. **10**, 3513 (1998).
[6] J. HUANG, Y. YANG, S. XUE, B. YANG, S. LIU, and J. SHEN, Appl. Phys. Lett. **70**, 2335 (1997).
[7] I. YU, T. ISOBE, and M. SENNA, J. Phys. Chem. Solids **57**, 373 (1996).
[8] R. JERKINS, W. F. MCCLUNE et al., Powder Diffraction File, JCPDS International Center for Diffraction Data, 1985.
[9] B. D. CULLITY, Elements Of X-Ray Diffraction, Addison-Wesley, Reading (Mass.) 1978 (p. 102).
[10] J. OUYANG, F. F. FANG, and A. J. BARD, J. Electrochem. Soc. **136**, 1033 (1989).
[11] W. G. BECKER and A. J. BARD, J. Phys. Chem. **87**, 4888 (1983).
[12] J. F. SUYVER, S. F. WUISTER, J. J. KELLY, and A. MEIJERINK, to be submitted.